Potent preclinical activity of FLT3-directed chimeric antigen receptor T-cell immunotherapy against *FLT3*-mutant acute myeloid leukemia and *KMT2A*-rearranged acute lymphoblastic leukemia

Lisa M. Niswander,[1*] Zachary T. Graff,[2,3*°] Christopher D. Chien,[4*] John A. Chukinas,[1] Christina A. Meadows,[3] Lillie C. Leach,[3] Joseph P. Loftus,[1] M. Eric Kohler,[2,3] Sarah K. Tasian,[1,5#] Terry J. Fry[2,3#]

[1]Children's Hospital of Philadelphia, Division of Oncology and Center for Childhood Cancer Research, Philadelphia, PA; [2]Center for Cancer and Blood Disorders, Children's Hospital Colorado, Aurora, CO; [3]Department of Pediatrics, University of Colorado Anschutz Medical Campus, Aurora, CO; [4]Pediatric Oncology Branch, Center for Cancer Research, National Cancer Institute, National Institutes of Health, Bethesda, MD and [5]University of Pennsylvania Perelman School of Medicine and Abramson Cancer Center, Philadelphia, PA, USA

°Current affiliation: Medical College of Wisconsin, Department of Pediatrics, Division of Hematology and Oncology, Milwaukee, WI, USA

[*]LMN, ZTG, and CDC contributed equally as co-first authors.
[#]SKT and TJF contributed equally as co-senior authors.

Correspondence:
S.K. Tasian
tasians@chop.edu
T.J. Fry
terry.fry@cuanschutz.edu

Received: May 24, 2022.
Accepted: August 3, 2022.
Prepublished: August 11, 2022.

https://doi.org/10.3324/haematol.2022.281456

SUPPLEMENTARY DATA

SUPPLEMENTAL METHODS

FLT3 chimeric antigen receptor construct design

FLT3 (CD135)-binding single-chain fragment variable (scFv) sequences were derived from publicly-available anti-CD135 NC7[1] and other antibodies. ScFv construct subcloning into a third-generation lentiviral plasmid (pENL-BBζ) containing a CD8 hinge and transmembrane domain, a 4-1BB (CD137)-signaling domain, and a CD3ζ costimulatory domain (**Figure 1A**) was performed as previously described.[2, 3] Multiple permutations of FLT3 scFvs and binding domain ordering were assessed to determine the optimal CAR construct for subsequent comprehensive *in vitro* and *in vivo* testing in preclinical leukemia models.[4]

Construction of CD19xFLT3 bicistronic chimeric antigen receptors

Bispecific CD19xFLT3 CAR constructs were based on a previously described CD19xCD22 CAR containing the CD19-binding scFv FMC63.[5, 6] Using CD19xCD22 CAR plasmid as a cloning vector, bicistronic constructs were designed using the selected FLT3 NC7 scFv with 4-1BB and CD3ζ costimulatory domains (BBz) paired with an FMC63 antibody CD19 scFv with either BBz or CD28 and CD3ζ domains (28z) (**Figure 5A**). The two CD3ζ and/or 4-1BB regions in the bicistronic constructs were optimized to avoid identical DNA sequences. CAR with BBz were designed with a CD8 hinge and transmembrane domain, and CAR with 28z were designed with a CD28 hinge and transmembrane domain. Monovalent CD19CART/BBz was used as a positive CAR T cell control for B-ALL studies.

Lentiviral vector production and T-cell transduction.

FLT3 and CD19xFLT3 CAR-encoding lentiviral supernatants were produced by transfection of the Lenti-X 293T cell line (Clontech) as previously described.[7, 8] Briefly, 293T cells

were transfected using Lipofectamine 3000 (Invitrogen) with plasmids encoding the CAR construct and retroviral packaging and envelope DNA (pMDLg/pRRE, pMD.2G, pRSV-Rev). Viral supernatant was harvested at 24 and 52 hours after transfection, centrifuged for 10 minutes at 3,000 rpm to remove cell debris, and snap frozen for storage at -80°C.

Human peripheral blood mononuclear cells from healthy donors were obtained via National Institutes of Health- or Children's Hospital Colorado-approved research protocols. T cells were isolated using EasySep Human T cell isolation kit (StemCell Technologies) and incubated at a 3:1 ratio with human CD3/CD28 Dynabeads (Gibco) in the presence of IL-2 (40 IU/mL, StemCell Technologies) for 48 hours. Activated T cells were resuspended in 1 mL at 2 million cells per 3 mL of lentiviral supernatant in the presence of protamine sulfate (10 μg/mL) and IL-2 (100 IU/mL) and centrifuged at 1000*g* for 2 hours at 32°C followed by incubation at 37°C in 10% CO2 for 24 hours, after which CD3/CD28 beads were removed. T cell expansion continued in AIM-V media supplemented with 5% heat-inactivated fetal bovine serum with 100 IU/ml IL-2 until harvest on day 9. Negative-control T cells (designated as 'mock T cells') were created in parallel with the omission of the CAR-containing transfer plasmid.

In vitro analysis of FLT3CART anti-leukemia activity

Cytotoxicity measurements and cytokine production were performed as previously described.[7, 8] Cytotoxicity was assessed *in vitro* by luciferase reporter assay (Promega) using luciferase-transduced human leukemia cell lines. Briefly, mock-transduced T cells, FLT3CART, CD19CART, or FLT3xCD19CART and target leukemia cells were co-incubated at 1:1 ratio. Cells were pelleted by centrifugation at 24, 48, 72, and 96 hours and analyzed via luciferase reporter assay per the manufacturer's instructions. Luminescence was measured with a Synergy 2 multi-detection plate reader (BioTek). Data were normalized to baseline (day 0) leukemia cell-only luminescence readings for each cell line.

To assay cytokine secretion, effector FLT3CART and target ALL or AML cells were co-incubated at 1:1 ratio for 48 hours. Human interleukin-2 (IL-2) and interferon-gamma (IFN-y) production was quantified in culture supernatants by ELISA (Biolegend).

ALL and AML patient-derived xenograft models for in vivo testing

Viably cryopreserved human leukemia and normal healthy bone marrow specimens from pediatric and/or adult patients were obtained from the leukemia biorepositories at the Children's Hospital of Philadelphia (CHOP), Children's Oncology Group (COG), and Penn via informed consent on research biobanking protocols in accordance with the Declaration of Helsinki. Patient-derived xenograft (PDX) leukemia models were established in NOD-scid IL2Rγ^{null} (NSG; Jackson Laboratories) mice for ALL specimens and in busulfan-conditioned (25 mg/kg intraperitoneally) NOD-*scid* IL2Rγ^{null}-3/GM/SF (NSGS; Jackson Laboratories) mice for AML specimens with serial transplantation for model expansion as previously described.[8-10] Secondary or tertiary leukemia PDX models were used for *in vivo* experimental FLT3CART and CD19xFLT3CART studies.

In vivo analyses of FLT3CART and CD19xFLT3CART functionality

For cell line xenograft model experiments, 6-8 week-old male or female NSG mice were injected intravenously (IV) with 5e5-1e6 luciferase-expressing ALL or AML cells. Leukemia burden was assessed for initial engraftment and then biweekly post-treatment via bioluminescent imaging (BLI) with IVIS Lumina Imaging System (PerkinElmer) and analyzed with Living Image software (PerkinElmer) as described.[8, 9] For PDX model studies, 1e5-1e6 viably cryopreserved secondary or tertiary murine spleen cells containing >80% human leukemia were injected into NSG mice (ALL specimens) or 2e6-5e6 cells into busulfan-conditioned NSGS mice (AML specimens). Once PDX mice demonstrated >1% human leukemia engraftment in peripheral blood, they were randomized to IV treatment with saline, mock-transduced T cells, or FLT3CART

at dosing indicated in figure legends. Animals were monitored by weekly retro-orbital venous blood sampling via quantitative FC analysis of CD45+/CD33+ human AML or CD45+/CD19+ human ALL cells and CD3+ T cells in peripheral blood and in end-study bone marrow and/or spleens as described (antibody list in Supplemental Methods).[8, 9] Endpoints for animal sacrifice and end-study analysis were based on the rate of ALL or AML progression in saline-treated control animals. For bispecific CAR T cell studies, additional cohorts of leukemia-engrafted mice were treated with CD19CART or CD19xFLT3CART and followed as above.

Flow cytometry analyses

Human ALL cells were identified with CD45-APC and CD19-APC-Cy7 antibodies, human AML cells with CD45-APC and CD33-APC-Cy7 antibodies, and human T cells with CD45-APC and CD3-eFluor450 antibodies (eBioscience or Invitrogen). Immunophenotypic markers of T cell activation and exhaustion were analyzed with CD25-FITC, CD71-FITC, PE-CD366 (TIM3), CD223-PE (LAG3), and PE-CD279 (PD-1) antibodies (eBioscience).

FLT3-CAR T cell surface expression was detected using an anti-G4S antibody (kindly provided by ElevateBio) with a PE-conjugated donkey anti-rabbit secondary antibody (BD Biosciences) or with biotin-conjugated protein L (ThermoFisher) and PE-Cy7 streptavidin (BD Biosciences) (**Supplemental Figure 3A**). CD19CART surface expression for the bispecific studies was detected with an AlexaFluor647-conjugated anti-CD19-Fc antibody (R&D Systems, Molecular Probes Protein Labeling Kit).

Human hematopoietic progenitor studies were performed with CD38-PerCP5.5 (BD Biosciences) and CD34-FITC, biotin-conjugated CD10, CD19, CD11b, CD8, CD4, CD56, CD20, and CD14 with streptavidin-conjugated Alexa Fluor 647 (ThermoFisher). A Zombie Violet dye was also used for viability assessment (Biolegend).

Assessment of in vitro on-target/off-tumor toxicity of FLT3CART

Tissue-specific human induced pluripotent stem cells (iPSCs) of cardiomyocytes, endothelial cells, hepatocytes, and central nervous system cells (glutaminergic neurons, GABA neurons, and astrocytes) were obtained from FujiFilm Cellular Dynamics (Madison, WI). Tissue-specific iPSCs were co-incubated 1:1 with FLT3CART for 16 hours based upon manufacturer's instructions, and culture supernatants were analyzed for IFN-γ production by ELISA as described to assess potential on-target/off-tumor reactivity against non-hematopoietic tissues.[8]

Potential hematopoietic toxicity of FLT3CART was assessed using viably-cryopreserved Ficoll-separated bone marrow mononuclear cells from deidentified normal adult HSCT donors obtained from the CHOP biorepository. CD34+ cells were isolated via an Aurora CS FC sorter (Cytek) and incubated without T cells, with mock-transduced T cells, or with FLT3CART for 18 hours in StemPro-34 serum-free medium (ThermoFisher). After co-incubation, cells were analyzed by FC to identify specific hematopoietic progenitor subsets (Supplemental Methods) or were plated in MethoCult H4034 Optimum (StemCell Technologies) for methylcellulose colony assays as per manufacturer's instructions. Plates were incubated at 37°C in 5% CO_2 for 14 days. Erythroid (BFU-E/CFU-E) and myeloid (CFU-G/GM/GEMM) colonies were counted on an inverted microscope (Nikon Eclipse).

Creation of NALM-6 antigen variant models

CRISPR-Cas9 technology was used to delete CD19 in luciferase-transduced NALM-6 cells as previously described,[5] and a FLT3-encoding lentiviral vector was then used to generate FLT3-overexpressing NALM-6 CD19+ and CD19- cell lines. Briefly, a murine IgG signal peptide followed by a truncated human FLT3 peptide was designed from sequences obtained by UniProt (UniProtKB). The amino acid sequences were reverse-translated, codon-optimized, and synthesized as a single construct (GeneArt, Life Technologies). This construct was subcloned into a third-generation lentiviral plasmid with sequence confirmation by Sanger sequencing. *FLT3*-encoding lentiviral vectors were then produced by transient transfection of the 293T cell line as

previously described.[5] Native CD19+ NALM-6 and CD19-deleted NALM-6 cells were transduced with human FLT3 lentiviral vector to generate the FLT3-overexpressing cell lines via addition of 1e6 leukemia cells/mL to 3 mL of EF1a-human FLT3 lentiviral supernatant in a 6-well plate. Spinfection was carried out at 1000*g* for 2 hours at 32°C, followed by incubation at 37°C for 24 hours. Cells were then replated at 2e5/mL and cultured at 37°C in 8% CO_2 (due to local altitude) for an additional 24 hours. Finally, the FLT3+/CD19+ and FLT3+/CD19- NALM-6 cells were sorted by flow cytometry for downstream experimental use in the bispecific CD19xFLT3CART studies.

SUPPLEMENTAL REFERENCES

1. Piloto O, Levis M, Huso D, et al. Inhibitory anti-FLT3 antibodies are capable of mediating antibody-dependent cell-mediated cytotoxicity and reducing engraftment of acute myelogenous leukemia blasts in nonobese diabetic/severe combined immunodeficient mice. Cancer Res. 2005;65(4):1514-1522.
2. Imai C, Mihara K, Andreansky M, et al. Chimeric receptors with 4-1BB signaling capacity provoke potent cytotoxicity against acute lymphoblastic leukemia. Leukemia. 2004;18(4):676-684.
3. Milone MC, Fish JD, Carpenito C, et al. Chimeric receptors containing CD137 signal transduction domains mediate enhanced survival of T cells and increased antileukemic efficacy in vivo. Mol Ther. 2009;17(8):1453-1464.
4. Chien CD, Sauter CT, Ishii K, et al. Preclinical Development of FLT3-Redirected Chimeric Antigen Receptor T Cell Immunotherapy for Acute Myeloid Leukemia. Blood. 2016;128(22):1072-1072.
5. Qin H, Ramakrishna S, Nguyen S, et al. Preclinical Development of Bivalent Chimeric Antigen Receptors Targeting Both CD19 and CD22. Mol Ther Oncolytics. 2018;11(127-137.
6. Maude SL, Frey N, Shaw PA, et al. Chimeric antigen receptor T cells for sustained remissions in leukemia. N Engl J Med. 2014;371(16):1507-1517.
7. Qin H, Cho M, Haso W, et al. Eradication of B-ALL using chimeric antigen receptor-expressing T cells targeting the TSLPR oncoprotein. Blood. 2015;126(5):629-639.
8. Qin H, Yang L, Chukinas JA, et al. Systematic preclinical evaluation of CD33-directed chimeric antigen receptor T cell immunotherapy for acute myeloid leukemia defines optimized construct design. J Immunother Cancer. 2021;9(9):
9. Tasian SK, Kenderian SS, Shen F, et al. Optimized depletion of chimeric antigen receptor T cells in murine xenograft models of human acute myeloid leukemia. Blood. 2017;129(17):2395-2407.
10. Loftus JP, Yahiaoui A, Brown PA, et al. Combinatorial efficacy of entospletinib and chemotherapy in patient-derived xenograft models of infant acute lymphoblastic leukemia. Haematologica. 2021;106(4):1067-1078.

SUPPLEMENTAL TABLES

Table S1. Genetic characteristics of human AML cell lines utilized in these studies.

AML cell line	Genetic alteration	*FLT3* mutation status
THP-1	t(9;11) with *KMT2A-MLLT3*	wild-type
MOLM-14	t(9;11) with *KMT2A-MLLT3*	heterozygous *FLT3*-ITD
MV4;11	t(4;11) with *KMT2A-AFF1*	homozygous *FLT3*-ITD

Table S2. Genetic characteristics of human ALL cell lines utilized in these studies.

ALL cell line	Genetic alteration	*FLT3* mutation status
NALM-6	t(5;12) with *ETV6-PDGFRB*	wild-type
HB11;19	t(11;19) with *KMT2A-MLLT1*	*FLT3* D835H
KOPN-8	t(11;19) with *KMT2A-MLLT1*	wild-type
SEM	t(4;11) with *KMT2A-AFF1*	*FLT3* amplification

Table S3. Molecular and cytogenetic characteristics of ALL and AML PDX models.

PDX model	COG USI	Disease status	*KMT2A* status	*FLT3* status	Translocation	Other genetic alterations
ALL185GD	PAVVRD	*de novo*	wild-type	wild-type	*P2RY8-CRLF2, PAX5-AUTS2*	*JAK2* R683G, *CDKN2A/B* del
ALL3113	n/a	*de novo*	*KMT2A-AFF1*	wild-type	t(4;11)(q21;q23)	*JAK2* mut, *TP53* del, *IKZF1* del
ALL3103	n/a	relapse	*KMT2A-MLLT3*	wild-type	t(9;11)(p21;q23)	none identified
ALL135MD	PAUYJT	*de novo*	*KMT2A-MLLT1*	wild-type	t(11;19)(q23;p13.3)	none identified
ALL2184*	n/a	*de novo*	*KMT2A-AFF1*	wild-type	t(4;11)(q21;q23)	*TP53* R282P, *TP53* R284G, *NRAS* Q61K and Q61R
AML2311*	n/a	relapse/ lineage switch	*KMT2A-AFF1*	wild-type	t(4;11)(q21;q23)	*TP53* R282P, *NRAS* Q61K and Q61R
AML11c	n/a	relapse	wild-type	*FLT3*-ITD, *FLT3* D835H	none identified	none identified
JMML117	n/a	*de novo*	wild-type	wild-type	none identified	monosomy 7, *PTPN11* G503V

COG USI = Children's Oncology Group unique specific identifier, del = deletion, mut = mutation, n/a = not available. *Paired lineage-switch leukemia samples from the same patient.

SUPPLEMENTAL FIGURES

Supplemental Figure 1. *In vivo* dose titration of FLT3CART in *KMT2A*-R ALL cell line xenograft model. (**A**) Schematic of FLT3CART chimeric antigen receptor construct containing single-chain variable fragment (scFv) from a commercially-available anti-CD135 antibody (clone NC7), CD8 hinge and transmembrane domains, 4-1BB costimulatory domain, and CD3ζ signaling domain. (**B**) Representative flow cytometry plot demonstrating FLT3 chimeric antigen receptor (CAR) construct transduction efficiency in human T cells by assessment of CAR surface expression with biotin-conjugated protein L, as described in the Supplemental Methods (**C**) Luciferase-expressing SEM cells (5e5) were injected IV vial tail vein into NSG mice on day 0. Once engraftment was documented by bioluminescent imaging (BLI) on day 14, mice were randomized to IV treatment with mock-transduced T cells (1e7/mouse) or FLT3CART (1e6, 5e6, or 1e7/mouse). Mice were followed by BLI at the designated time points. FLT3CART cell dose-dependent decrease inhibition of *in vivo* SEM cell leukemia proliferation was detected with curative effects seen at higher cell dosing.

Supplemental Figure 2. FLT3CART does not inhibit *in vivo* leukemia proliferation in FLT3-negative *KMT2A* wild-type ALL. (**A**) Flow cytometry assessment of FLT3 site density (molecule/cell) on iALL185GD ALL PDX cells derived from an infant ALL patient harboring a *P2RY8-CRLF2* fusion is shown relative to other PDX models used in these studies. FLT3 expression for this non-*KMT2A*-R ALL (light green) is below the level of quantification and is shown in parallel with FLT3 site density already displayed in **Figures 3 and 4** for *FLT3*-mutant AML (dark blue), *FLT3* wild-type AML (light blue) and *KMT2A*-R ALL (dark green) PDX samples. (**B**) Once human leukemia was detectable at ≥1% in murine peripheral blood of iALL185GD PDX mice, animals were randomized (n=5/group) to IV treatment with 1e6 (dark blue), 5e6 (light blue), or 1e7 (turquoise) FLT3CART, mock-transduced T cells (green), or saline (yellow). CD19+CD45+

ALL (first panel) and CD3+CD45+ T cells (second panel) were quantified in spleens by flow cytometry at end of study, which was determined by rate of ALL progression in control mice (4 weeks post-treatment). No appreciable *in vivo* FLT3CART expansion was detected in peripheral blood (not shown) or in end-study murine spleens, and no reduction in human ALL burden was accordingly observed in murine spleens at any FLT3CART dose tested. Data are displayed as +/- standard error of the mean and were analyzed by one-way ANOVA with Dunnett's post-test for multiple comparisons. No significance was noted compared to mock T cell control group (ns).

Supplemental Figure 3. FLT3CART induces minimal on-target/off-tumor effects upon normal non-hematopoietic tissues. Human induced pluripotent cells (iPSCs) differentiated into normal tissue cell types as shown were co-incubated *in vitro* with FLT3CART at 1:1 E:T ratio (100,000 cells). IFN-γ production in supernatant was measured by ELISA. A small amount of IFN-γ production was induced by FLT3CART co-incubation with cardiomyocyte iPSCs, but was >25-fold lower than the amount produced with co-incubation of FLT3CART with FLT3+ MOLM-14 positive control cells. Data were analyzed by one-way ANOVA with Tukey's post-test for multiple comparisons with significance compared to mock T cell group for each experiment. Absence of symbol indicates lack of statistical significance. ****$p<0.0001$.

Supplemental Figure 4. No detectable FLT3CART activity against human CD34+ hematopoietic progenitors. (A) CD34+ cells were flow cytometry-sorted after thaw of viably-cryopreserved human bone marrow mononuclear cells; 1,000 CD34+ cells were co-cultured alone or with 1:1 ratio of mock-transduced T cells or FLT3CART for 20 hours, then suspended in cytokine-supplemented methylcellulose and incubated for 14 days. Erythroid (CFU-E), granulocyte-macrophage (CFU-GM), or mixed erythroid-myeloid (CFU-CEMM) colonies were quantified by 40x total magnification on inverted microscope. There was no difference in total

colony number or in the CFU subsets, indicating no detected on-target/off-tumor effects of FLT3CART upon hematopoietic colony formation. Data are displayed as +/- standard error of the mean for mean of n=3 human bone marrow donors with duplicate technical replicates. **(B)** CD34+ cells were flow sorted after thaw of viably-cryopreserved human bone marrow mononuclear cell samples (n=2) 10,000 cells were co-cultured as above alone or with 1:1 ratio of mock-transduced T cells or FLT3CART for 20 hours. Cytokine production (IL-2 and IFN-γ) in co-culture supernatant after 20 hours was measured by ELISA. Production of IL-2 and IFN-γ from FLT3CART was detected when co-incubated with positive control MOLM14 AML cell line, but not when cultured with primary CD34+ hematopoietic progenitors. (**C**) After 20 hours, cells in co-culture were analyzed with flow cytometry to quantify CD34+ hematopoietic progenitor subsets subdivided by CD38+ and CD38-. Gating strategy for a representative sample displays cells first gated on live (negative for Zombie Violet), single cells (FSC-A versus SSC-A, FSC-A versus FSC-H), non-lineage-committed (negative for CD10, CD19, CD11b, CD8, CD4, CD56, CD20, CD14) prior to identifying CD34+ cells as CD38+ or CD38-. (**D**) Progenitor subsets for CD34+ cells co-cultured alone or with mock T cells or FLT3CART were quantified with CountBright absolute counting beads (ThermoFisher) and are displayed as percent of no T cell control cultures. There was no difference in number of CD34+CD38- or CD34+CD38+ hematopoietic progenitors following exposure to FLT3CART. Data in (A) were analyzed by one-way ANOVA with Tukey's post-test for multiple comparisons with significance compared to mock T cell group. Absence of symbol indicates lack of statistical significance. Data in (D) are presented as mean of 2 donor bone marrow samples +/- standard deviation.

Supplemental Figure 5. Validation of bicistronic CD19xFLT3CART CAR T cells. (**A**) Human T cells were transduced with bicistronic CD19(28z)xFLT3CART and CD19(BBz)xFLT3CART vectors as described in Supplemental Methods. Cell surface CD19CAR was detected by fluor-

conjugated anti-CD19-Fc and FLT3CAR expression detected by anti-G4S with secondary antibody as described in Supplemental Methods. Flow cytometry demonstrates T cells expressing both CD19CAR and FLT3CAR from a single vector bicistronic CAR construct. **(B)** CD19 and FLT3 single and double antigen-expressing NALM-6 B-ALL cells were created for validation of bicistronic CD19xFLT3CARTs. CRISPR-Cas9 gene editing was used to delete native CD19 from NALM-6 and/or a FLT3-encoding lentiviral vector was used to express FLT3 to generate parental NALM-6 (CD19+FLT3-), CD19- NALM-6 (CD19-,FLT3-), FLT3+ NALM-6 (CD19+,FLT3+) and combined CD19- FLT3+ NALM-6. Modified variant antigen NALM-6 cell lines were co-incubated with mock-transduced T cells, monovalent FLT3CART (light blue), monovalent CD19CART (dark blue), CD19(28z)xFLT3CART (purple), or CD19(BBz)xFLT3CART (pink) in 1:1 ratio (100,000 cells). Cytokine production in culture supernatant was analyzed by ELISA. Dual-expressing CD19xFLT3CARTs production of IL-2 and IFN-γ was similar or greater with than monovalent CD19CART or FLT3CART. Data are displayed as +/- the standard error of the mean and are representative of $\geq$2 independent experiments.

Supplemental Figure 6. Co-culture with FLT3+ leukemia cells induces T cell activation marker expression on monovalent FLT3CART and bispecific CD19xFLT3CARTs *in vitro*. Mock-transduced T cells, monovalent FLT3CART (light blue), monovalent CD19CART (dark blue), CD19(28z)xFLT3CART (purple), or CD19(BBz)xFLT3CART (pink) were incubated in the absence (solid bars) or presence (lined bars) of SEM B-ALL cells in 1:1 ratio for 24 hours. Induction of CD25 (**A**) or CD71 (**B**) surface expression on CD4+ (left panels) and CD8+ (rights panels) T cells was evaluated by flow cytometry analysis. Quantification of median fluorescent intensity for CD4+ and CD8+ T cell subsets with n=3 technical replicates for each condition is displayed graphically +/- standard deviation. CD19xFLT3CARTs and monovalent FLT3CART exhibit similar upregulation of cell surface T cell activation markers CD25 and CD71 on both CD4+

and CD8+ T cells when co-incubated with FLT3-expressing leukemia cells. Basal, unstimulated bispecific CD19xFLT3CARTs displayed a small but significant elevation CD25 and CD71 expression compared to unstimulated Mock T cells. Statistical analysis was performed with one way ANOVA with Šidák's post-test for multiple comparisons. *p<0.05, **p<0.01, ***p<0.001, and ****p<0.0001, ns = not significant.

Supplemental Figure 7. Co-culture with FLT3+ leukemia cells induces T cell inhibitory receptor expression on monovalent FLT3CART and bispecific CD19xFLT3CARTs *in vitro.* Mock-transduced T cells, monovalent FLT3CART (light blue), monovalent CD19CART (dark blue), CD19(28z)xFLT3CART (purple), or CD19(BBz)xFLT3CART (pink) were incubated in the absence (solid bars) or presence (lined bars) of SEM B-ALL cells in 1:1 ratio for 24 hours. Induction of inhibitory T cell receptors PD-1 (**A**) TIM3 (**B**) and LAG3 (**C**) surface expression on CD4+ (left panels) and CD8+ (rights panels) T cells was evaluated by median fluorescent intensity flow cytometric analysis. CD19xFLT3CARTs and monovalent FLT3CART exhibit similar upregulation of cell surface T cell inhibitory receptors on both CD4+ and CD8+ T cells when co-incubated with FLT3-expressing leukemia cells. Interestingly there is a small but statistically significant increase in PD-1 staining on unstimulated bicistronic CD19xFLT3CARTs compared to unstimulated Mock T cells that is not present for monovalent FLT3CART or CD19CART. Statistical analysis was performed with one way ANOVA with Šidák's post-test for multiple comparisons. *p<0.05, **p<0.01, ***p<0.001, and ****p<0.0001, ns = not significant.

Supplemental Figure 8. Bispecific CD19xFLT3CART inhibits *in vivo* leukemia proliferation in ALL and AML cell line xenograft models. NSG mice were engrafted with luciferase-transduced (**A**) SEM *KMT2A*-R ALL cells or (**B**) MOLM14 *FLT3*-ITD AML cells and treated with saline, mock-transduced T cells, monovalent CD19CART, FLT3CART, or bicistronic

CD19xFLT3CARTs as described and summarized in **Figure 7A and 7B**. Bioluminescent imaging radiance assessment over time is shown visually for SEM and MOLM14 xenograft models.

Supplemental Figure 1

A

B

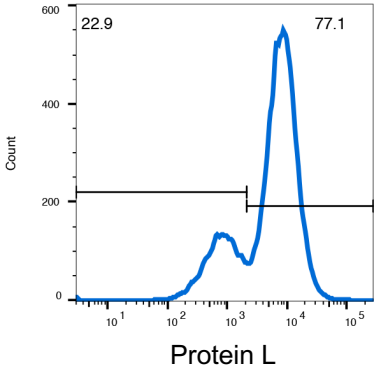

C

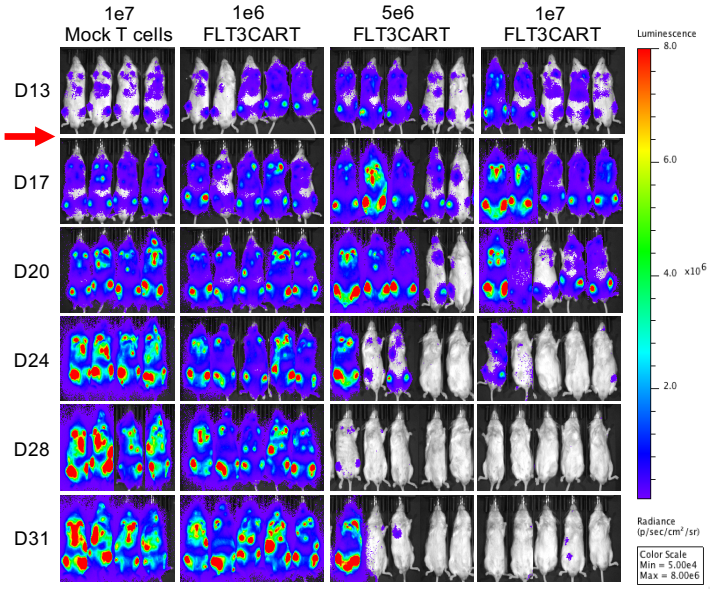

Supplemental Figure 2

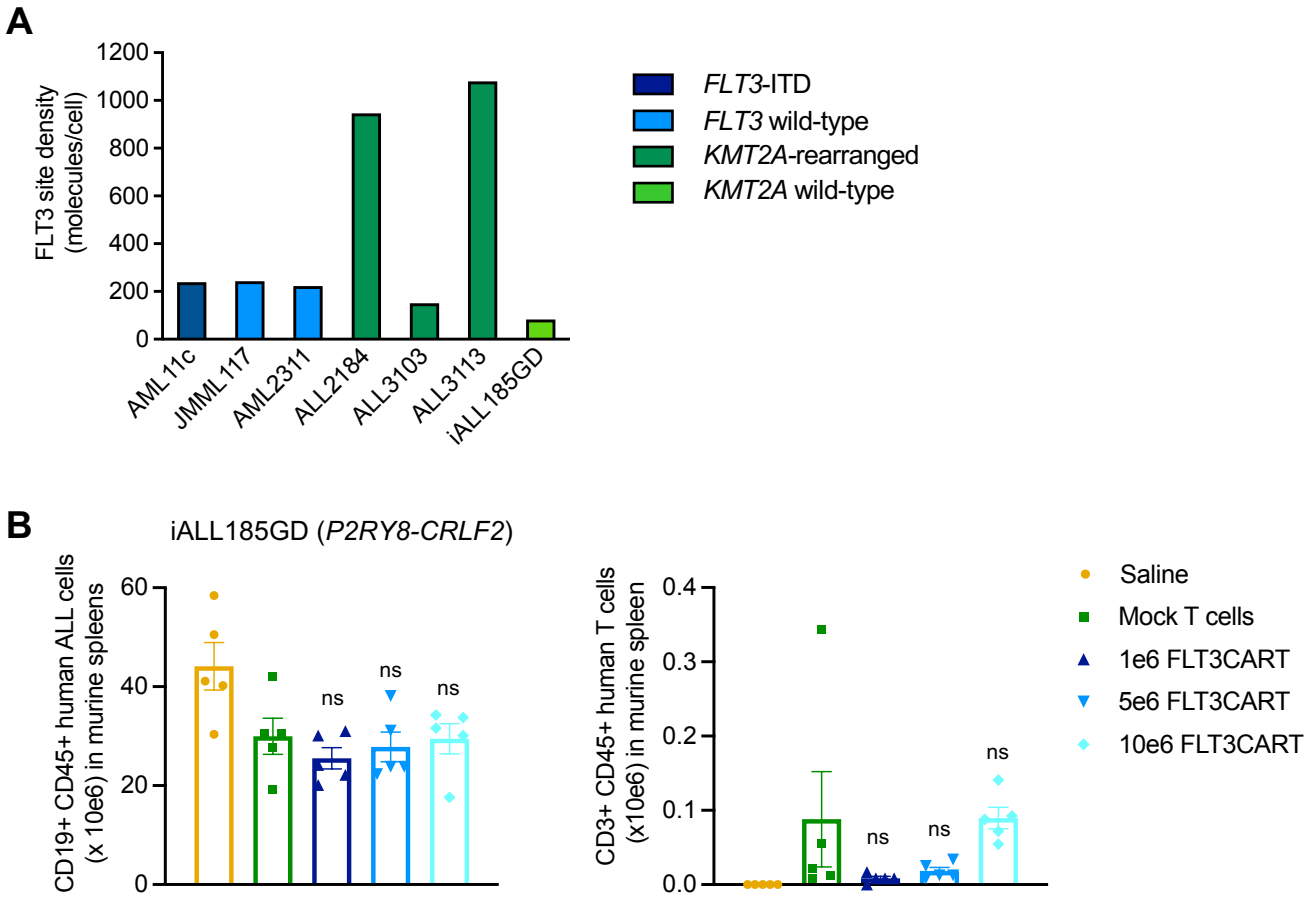

Supplemental Figure 3

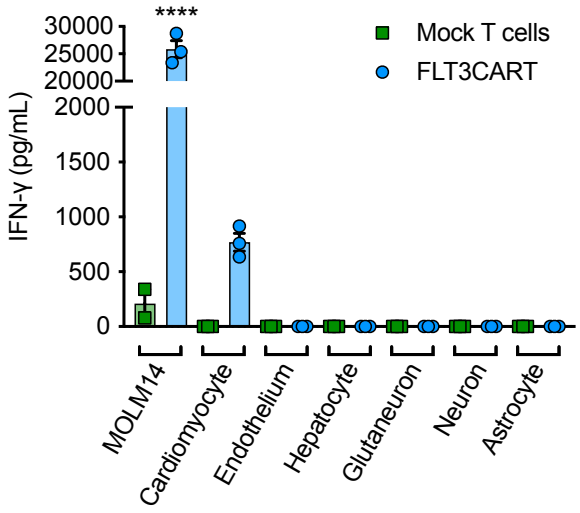

Supplemental Figure 4

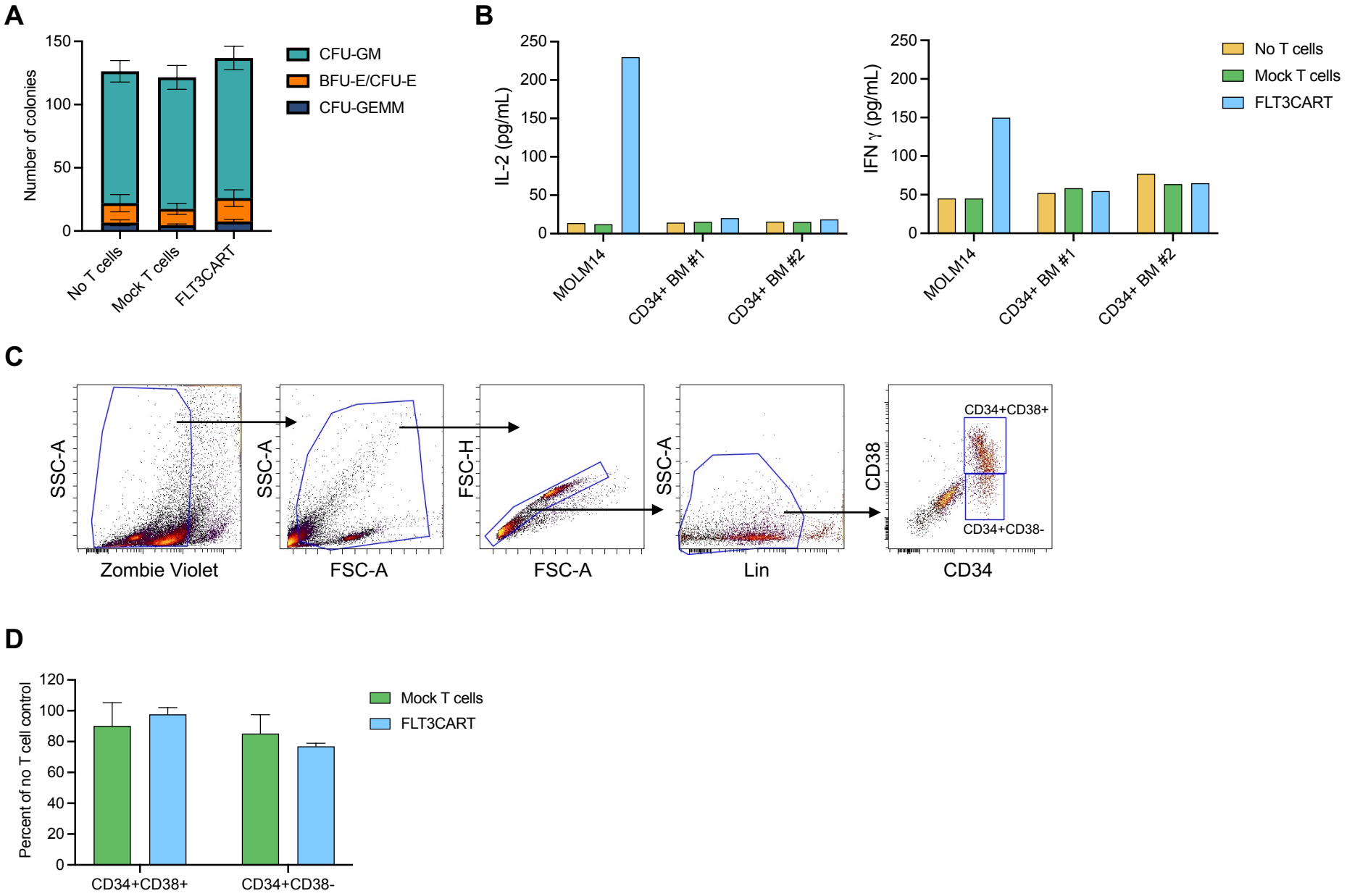

Supplemental Figure 5

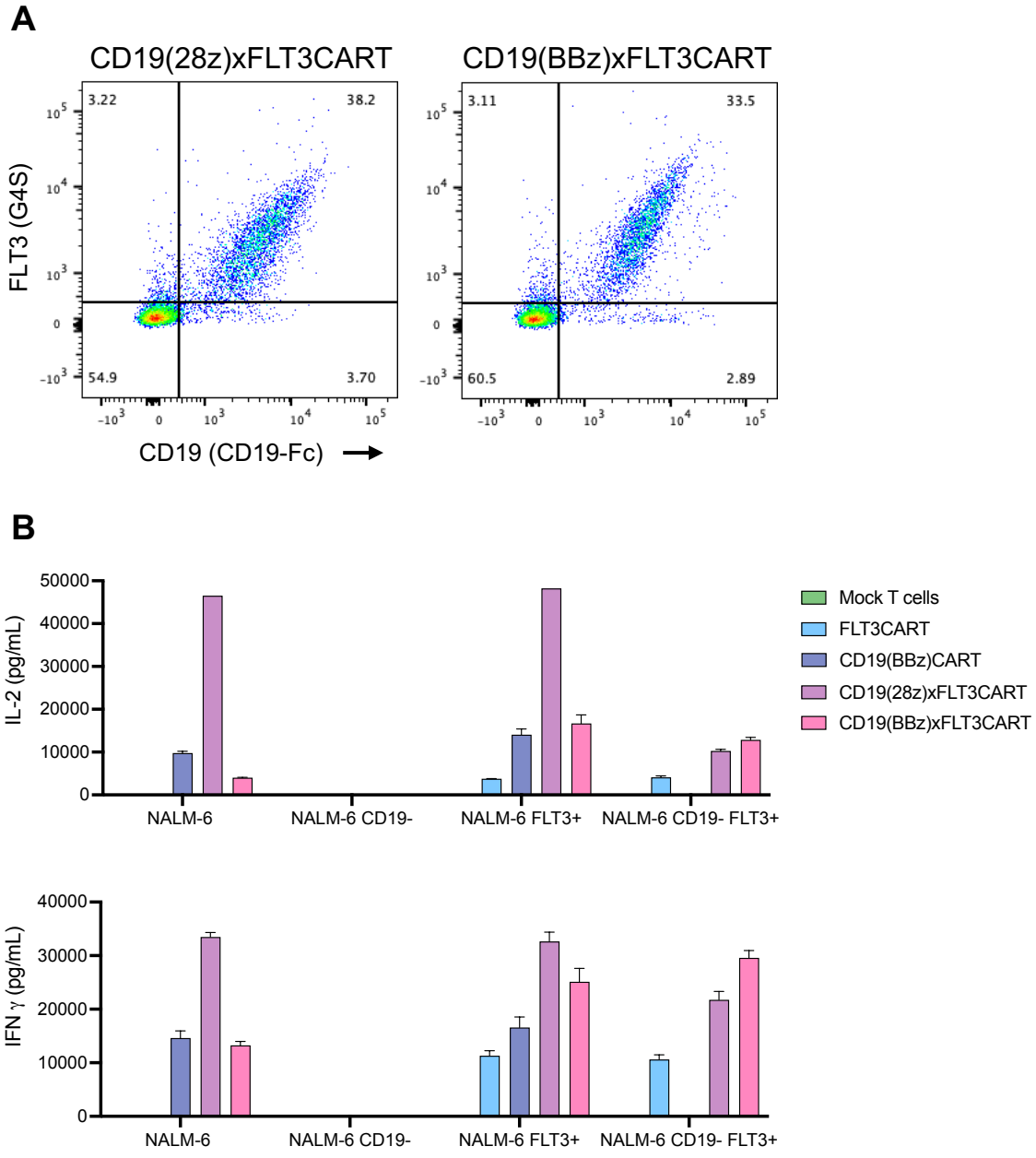

Supplemental Figure 6

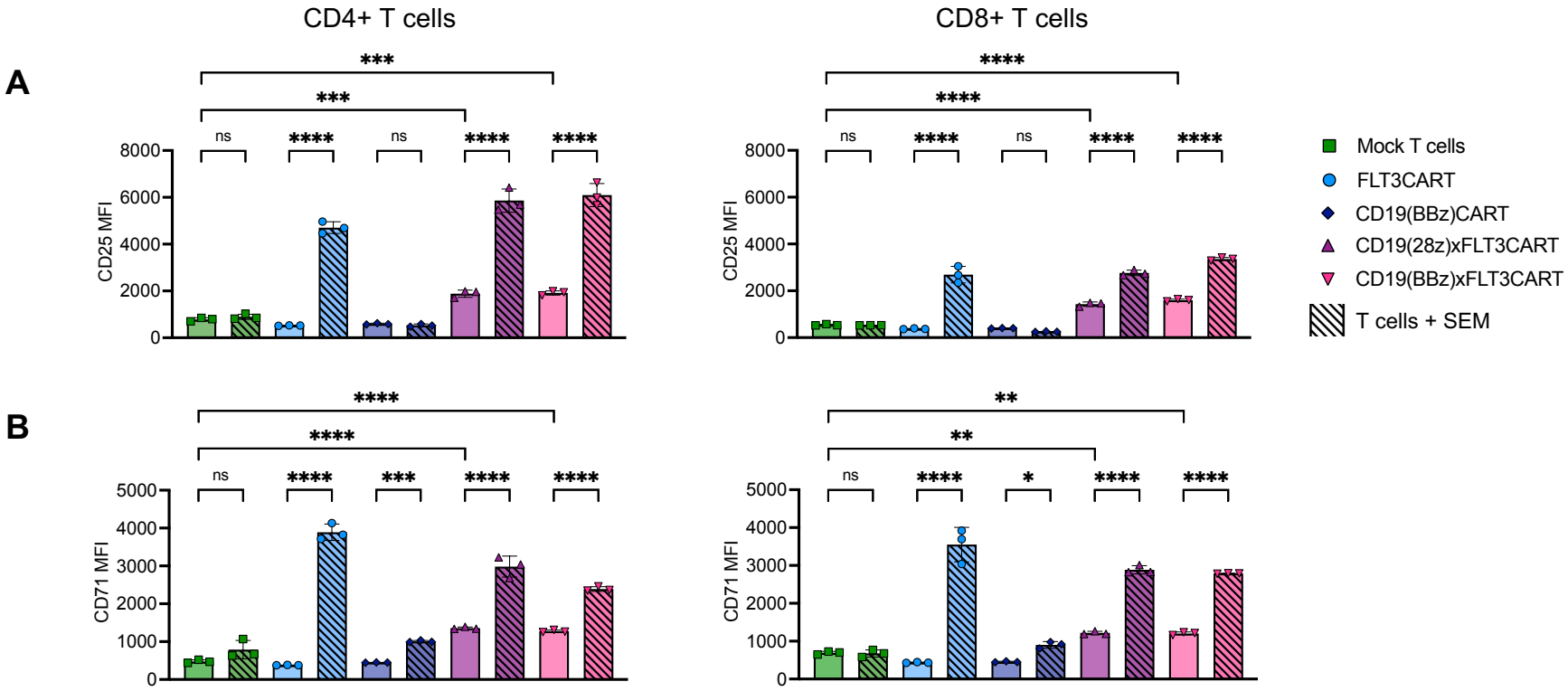

Supplemental Figure 7

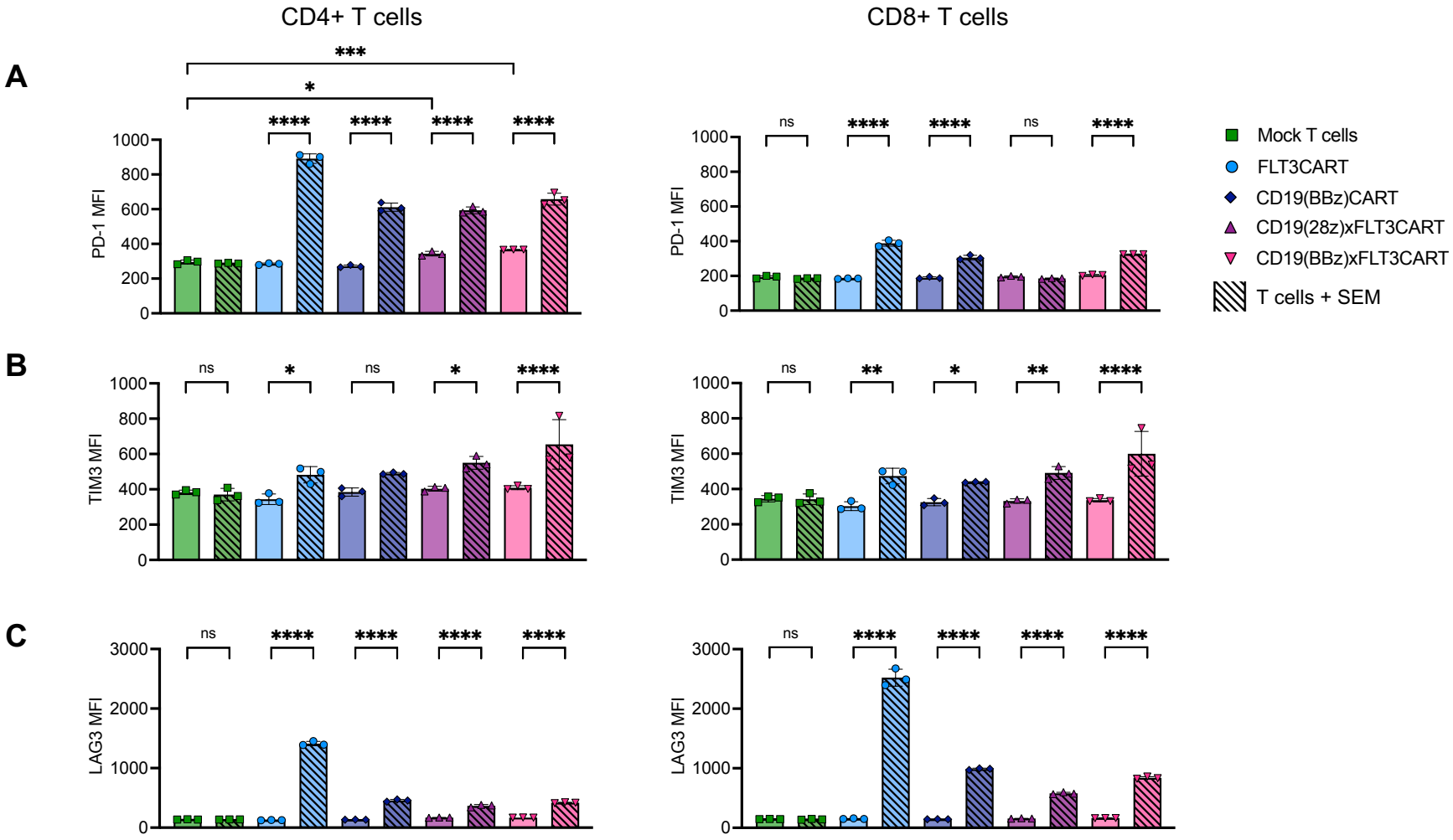

Supplemental Figure 8